Building Serv. Eng. Res. Technol. **15**(2) 81–93 (1994) Printed in Great Britain

Summary In hot climates ventilation can be a useful means of cooling dwellings, if the outside air is cooler than that inside the dwelling. Often, in hot regions the outside air is so hot during the day that cooling by ventilation is of no benefit until the evening when the outside air cools. Ventilation can then be beneficial, and can be promoted by a sun-warmed cavity or 'solar chimney' added to a building on the sunward side. The cavity may be of any material of high thermal capacity. Heat from the sun is stored within the walls and heats the air within. The cavity is closed at the top and bottom by dampers. These, when opened in the evening, allow the buoyant hot air contained within to rise, drawing cooler outside air into the building. This process continues until the stored energy is consumed. The performance of a typical cavity in inducing ventilation into a house is studied experimentally and theoretically. The measurements are made on a full-scale model under steady-state conditions. Cavity width and air inlet area are important parameters in this study. Measurements are made on the temperature and velocity of the air. Observations on air flow patterns in the room and the cavity are made. A dynamic model is developed based on a finite-difference technique, and used to examine the performance of the cavity in various circumstances. The results show that air movement can be produced by a sun-warmed cavity if the dimensions of inlet and cavity width are kept to certain values, and that thermal comfort can be improved.

Solar chimney for promoting cooling ventilation in southern Algeria

A Bouchair Arch PhD
Departement de Technologie, E.N.S. de JIJEL, Ouled Aissa, JIJEL 18000, Algeria

Received 25 October 1993, in final form 14 January 1994

List of symbols

A	Area (m^2)
c	Specific heat capacity ($J\,kg^{-1}\,K^{-1}$)
C_v	Ventilation conductance ($m^2\,K\,W^{-1}$)
g	Gravitational acceleration ($9.8\,m\,s^{-2}$)
h_c	Convection heat transfer coefficient ($W\,m^{-2}\,K^{-1}$)
h_r	Radiation heat transfer coefficient ($W\,m^{-2}\,K^{-1}$)
M	Mass flow rate ($kg\,s^{-1}$)
R	Thermal resistance ($m^2K\,W^{-1}$)
t	Time (s)
T	Temperature (°C)
x	Distance (m)
v	Velocity ($m\,s^{-1}$)
V	Volume (m^3)
W	Cavity width (m)
Y	Cavity length (m)
Z	Height of the cavity (m)

Greek symbols

ρ	Density ($kg\,m^{-3}$)
∂	Differential
λ	Thermal conductivity ($W\,m^{-1}\,K^{-1}$)
Δ	Difference

Subscripts

a	Air
ac	Cavity air
so,wm	Between outside surface node and the node in the middle of the wall
ao	Outside air
ar	Room air
eo	Outside environment
gr	Ground
si	Inside surface
sm	Mean surface
so	Outside surface
t	Present time
$t+1$	Future time
s	Surface
wm	Middle of a wall
mr	Mean radiant
res	Resultant

1 Introduction

Thermal comfort in buildings is arguably the most important factor for builders and designers to achieve. Unlike in cold climates such as Northern Europe, where heat conservation is most required to combat cold weather, in hot arid climates heat causes discomfort and cooling is the major need.

In warm climates, a dwelling may be cooled during summer by cross-ventilation through doors or windows because the outside air is not very hot. However, this cannot be the case for hot climates because the air outside is too hot. In the evening and during the night, the temperature of the outside air drops, and thus it can be used for cooling ventilation. Yagoubi and Golneshan[1] showed that encouraging ventilation at night and discouraging it during the day could be a useful way of achieving comfort in hot summers. A rate of 12 air changes per hour could be achieved by cross ventilation using wind towers. However, in urban areas air movement may be very restricted by building layout so that wind towers may be of benefit only if built high enough, and this may be too expensive. Moreover, there are cases where the wind speed at night is very low, and thus cooling by ventilation is limited. It is of interest therefore to study ways in which night ventilation could be improved by simple and inexpensive means, by taking advantage of day and night conditions as experienced in hot arid climates. The comfort temperature or 'dry resultant temperature' in a hot arid climate suggested by the *CIBSE Guide*[2] is of the order of 28°C with low air movement, but Nicol[3] has shown that thermal comfort

can be achieved with warmer conditions if the air velocity is about 0.25 m s^{-1}. He observed in India and Baghdad that 80% of people were comfortable at a resultant temperature up to 36°C.

1.1 Comfort in Southern Algerian housing

Thermal comfort in dwellings depends upon various environmental factors such as air temperature, mean radiant temperature, relative humidity and air movement. The range of conditions within which the majority of people would feel comfortable is called the 'Comfort zone'[4]. Various thermal index scales have been developed to express the base conditions. These indices are discussed in detail in references such as Evans[5]. Olgay[6] constructed a bioclimatic chart from which the comfort zone is defined in terms of relative humidity and air temperature. The lower and upper limits of thermal comfort in still air are 20–30°C respectively. Within this temperature range the relative humidity lies between 20–50%. As relative humidity increases above 50%, the upper limit of the comfort zone decreases. Thus the maximum air temperature for comfort appears to be less than 30°C. In places where the air temperature is higher than 30°C, thermal comfort can be improved by improving the air movement.

In hot climates such as that of El-Oued, the relative humidity in summer goes up to 50% in the early hours of the morning; this is within the comfort zone[7]. At night and early morning, the air temperature is low and is within the comfort zone; consequently, ventilation at night to improve thermal comfort would be desirable. However, the bioclimatic chart does not include the mean radiant temperature, which is an important environmental factor that affects thermal comfort. The *CIBSE Guide*[2] suggests an index to express thermal comfort which takes into account air velocity, mean radiant temperature and air temperature. It is called 'dry resultant temperature'. It is usually recorded by a globe thermometer placed in the centre of a room. The dry resultant temperature is used as index to indicate comfort in cold climates but it is also suitable for hot climates. The dry resultant temperature is given by:

$$T_{res} = \frac{T_{mr} + T_a(10v)^{0.5}}{1 + (10v)^{0.5}} \quad (1)$$

where T_{res} is the dry resultant temperature (°C), T_{mr} is the mean radiant temperature (°C), T_a is the air temperature (°C), v is the air velocity (m^{-1}).

1.2 The present work

It is intended in this study to investigate ways of improving thermal comfort inside dwellings by increasing ventilation in the evening. One way of achieving this is by using a sun-warmed cavity or 'solar chimney' constructed of stone, concrete or any other material of high thermal capacity. It can be added to an existing building or made by modifying a cavity wall such as is often used for thermal insulation. The cavity is to have dampers at the top and bottom which are closed throughout the day, so that it is passively heated. In the evening the dampers and the windows of the room are opened to permit ventilation. The air within the cavity flows upward by buoyancy, thus drawing cool outside air into the room through the windows. The air entering the cavity will take up heat stored from the walls to prolong the upward

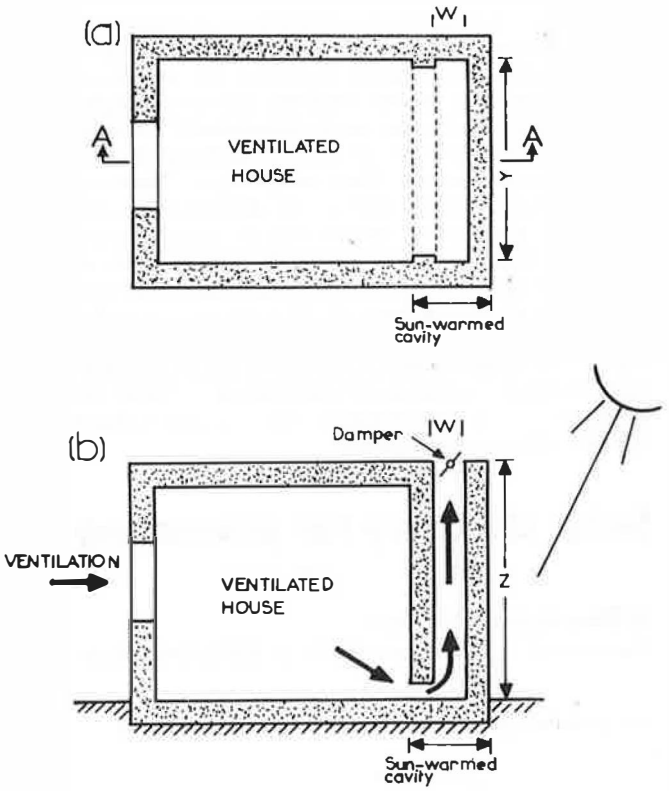

Figure 1 The proposed design: (a) Plan (b) Section A–A

flow. It is attempted to develop a sun-warmed cavity or a 'solar chimney' which is used to encourage air speeds through a room of 0.25 m s^{-1} as suggested by Nicol[3] to reduce the resultant temperature inside a building to a comfortable level. When the incoming air is cool and is moving, it will lower the air temperature and the mean radiant temperature of a room. This naturally will cool the cavity and the design must ensure that the rate of cooling is such that ventilation will continue for as long as is required. The cavity design is of length Y, width W and a height Z (Figure 1).

Air movement in a sun-warmed cavity is tested in the laboratory. The temperature of the cavity is varied to cover the possible range of temperature experienced in hot dry climates. The air flow and heat transfer processes are analysed and examined. The effects of cavity width and inlet height on the performance of the cavity and air flow patterns are assessed.

2 Experimental results

The monitoring equipment used for the measurements was described at length in References 7, 8 and 9. Tests were performed to find out the optimum dimensions of a cavity to produce maximum ventilation rates. The ambient air temperature in the laboratory was 20°C. The following parameters were varied: cavity width, inlet height, and surface temperature (T_{sm}) of the cavity.

2.1 Effect of cavity width

To study the effect of cavity width on the rate of mass flow, the cavity width was varied at the following intervals; 0.1 m, 0.2 m, 0.3 m, 0.5 m and 1.0 m. The surface temperature of the cavity walls was varied between 30°C and 60°C at 10 K intervals and each spacing, and the mass flow rates were monitored and calculated for unit

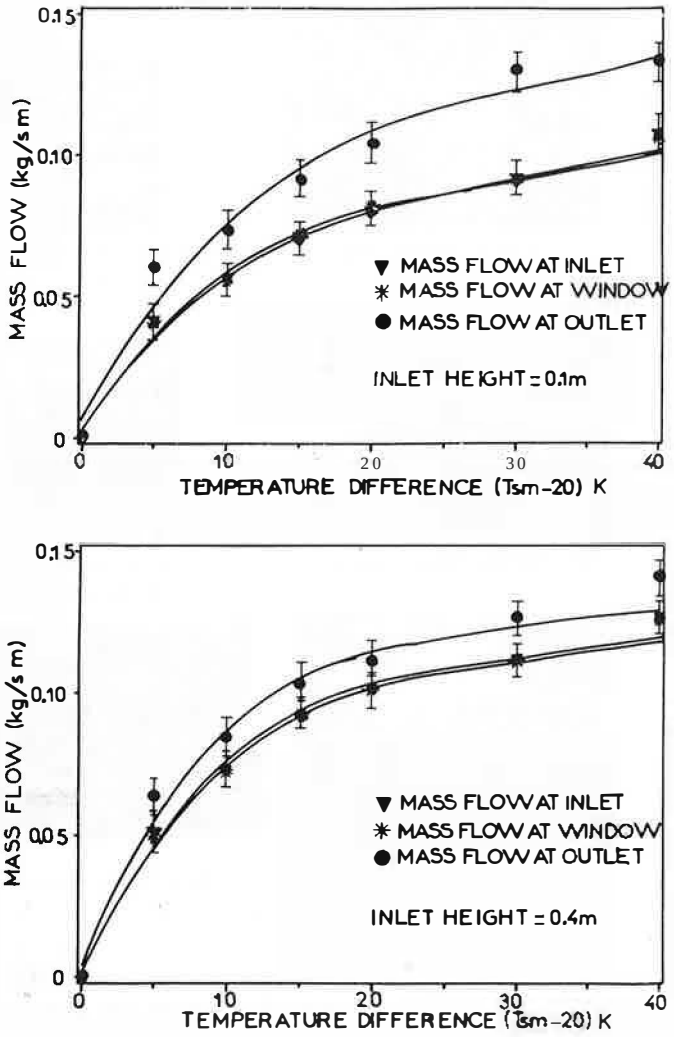

Figure 6 Mass balance for 0.5 m wide cavity

due to diminution of pressure loss, and also the down flow becomes less.

2.4 Discussion

As was stated earlier, thermal comfort can be improved if sufficient air movement is allowed over the body. Nicol[3] showed that 80% of a population feel comfortable with a resultant temperature between 32 and 36°C providing that the air speed past the human body is of the order of $0.25\,m\,s^{-1}$. From Figure 4, when the cavity is 0.2 m wide and the inlet is 0.1 m high, for a temperature difference between the internal surfaces of the cavity and the ambient air of 5 K, a mass flow in the order of $0.043\,kg\,s^{-1}$ is achieved.

If the cavity is 2 m high by 3 m long the mass flow rate would be $0.043 \times 3 = 0.13\,kg\,s^{-1}$, giving an average air velocity across the room (The air moves in a stream line from the window of the room to inlet of the cavity, as was observed.): $v = M/\rho A = 0.13/[1.2(0.5 \times 0.6 + 0.1 \times 3)/2] = 0.36\,m^{-1}$, where A is the mean area of the window and the inlet (m^2) and ρ is the air density. This is not far from the value suggested by Nicol[3].

With an air velocity of $0.36\,m\,s^{-1}$, the dry resultant temperature will be $T_{res} = 0.34T_{mr} + 0.65T_a$.

If we assume a mean radiant temperature of 37°C and ambient air at 28°C, the dry resultant temperature will be

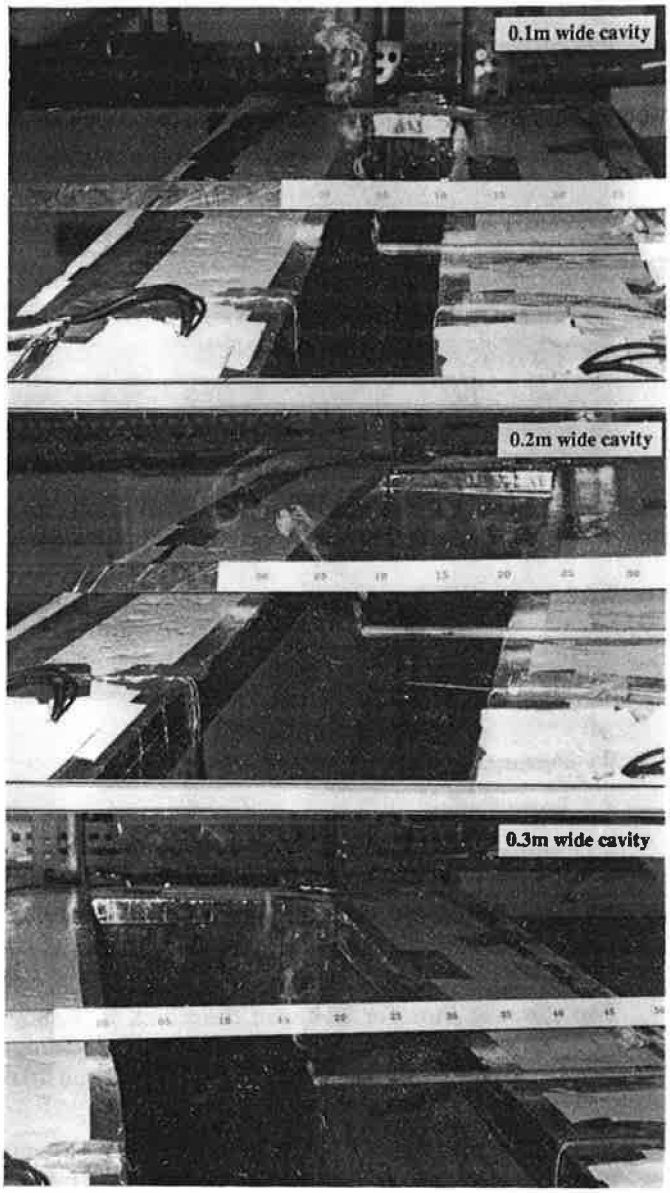

Figure 7 Air flow patterns at top of cavity

about 31°C. According to Nicol[3] this is quite comfortable.

For a temperature difference of the order of 40 K a mass flow rate of $0.113 \times 3 = 0.339\,kg\,s^{-1}$ is achieved, giving an air speed $v = 0.339/[1.2(0.5 \times 0.6 + 0.1 \times 3)/2] =$

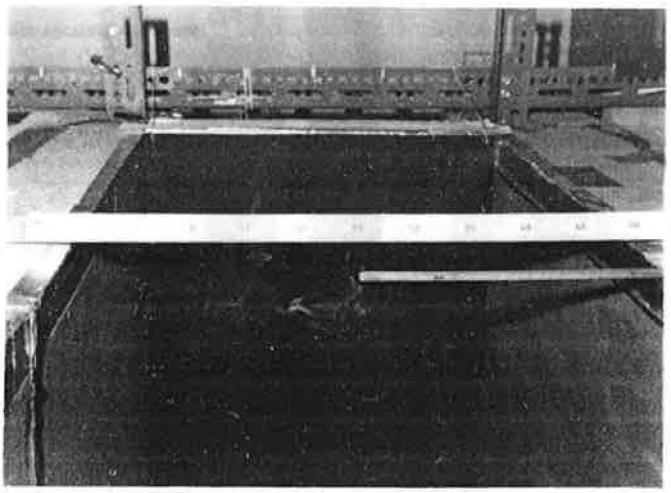

Figure 8 Downflow in the centre of a 0.5 m wide cavity

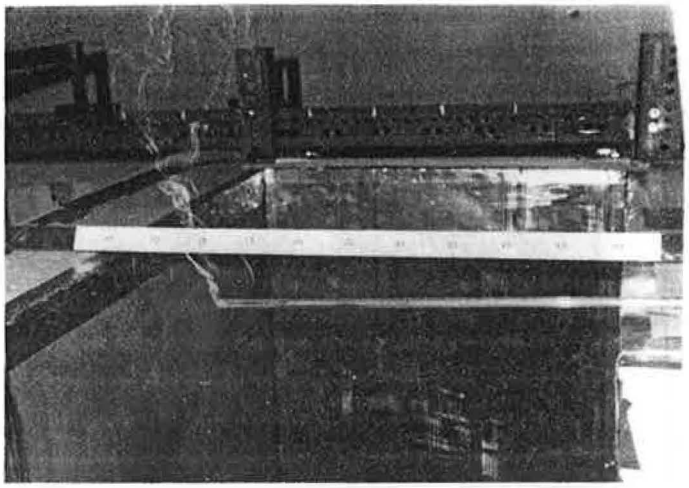

Figure 9 Upward flow near the surface of movable wall

$0.94\,m\,s^{-1}$ which would improve thermal comfort. For higher cavities, the mass flow will be greater. The height of the cavity in practice is limited to the height of the building.

3 Dynamic model

3.1 Introduction

The dynamic model developed in the current study was based on a numerical solution of the Fourier equation for transient heat flow in the building fabric. Heat balance equations were used in conjunction with the boundary conditions, for which a computer program was written.

The climatic data for El-Oued described in Reference 7 were used in the model. The external wall thicknesses of the cavity 'external leaf' were 0.05 m, 0.10 m, 0.15 m and 0.20 m.

The choice of azimuth is subjected to many considerations, including topography, sources of noise and wind

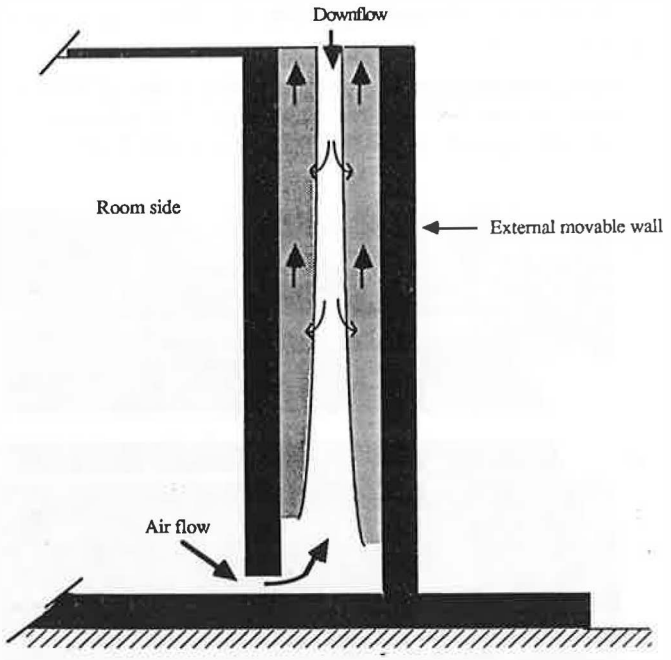

Figure 10 Schematic diagram of possible air flow patterns inside the cavity

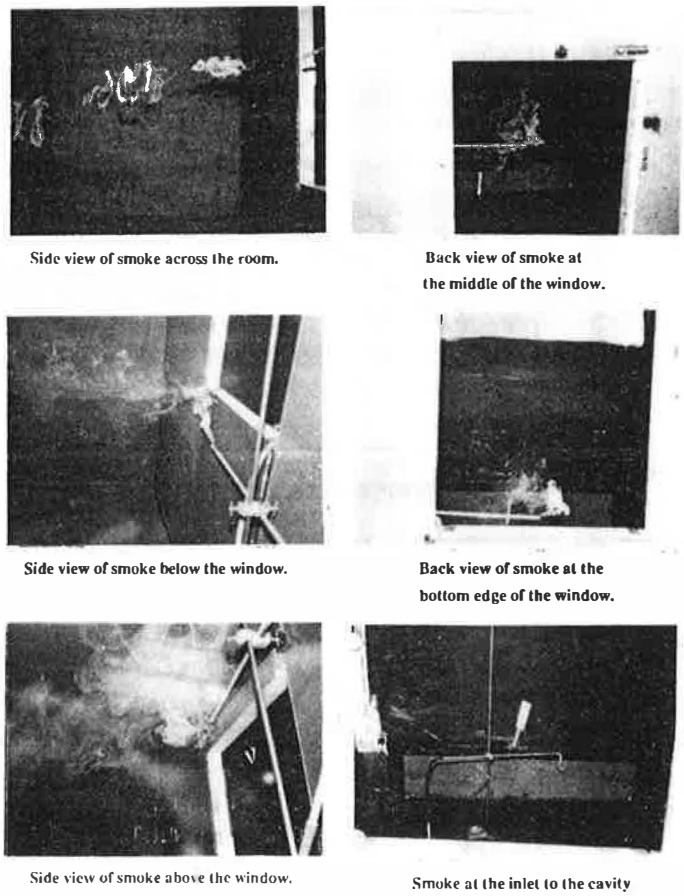

Figure 11 Airflow patterns in the room

direction. Attention in this study is given to solar radiation and its effect through heating on the performance of the cavity facing different directions.

Calculations were made for azimuths East, South and West. Cavity ventilation was assumed from 2000, 2200, and 2400 h to 1000 h and from 2000 h to 0800 h.

3.2 The model and assumptions

The model considered here is shown in Figure 14. It is a cubic room (3 m × 3 m × 3 m) with concrete walls 0.30 m thick, roof and floor 0.20 m thick, and a 3 m high cavity with an external leaf of variable outer thickness. The air cavity was 0.20 m wide. For simplicity, the calculations were performed assuming homogeneous materials and their assumed properties are presented in Table 1.

The temperature of the ground at a depth of 0.60 m was considered constant, at the monthly average outside air temperature.

Solar heat gain through windows was considered negligible because the windows are shuttered during the day and not usually facing the sun. Radiation loss from the

Table 1 Material properties used in the dynamic model

Parameter	Location			
	Walls	Roof	Floor	Air
Thermal conductivity ($W\,m^{-1}\,K^{-1}$)	1.1	0.2	1.1	0.027
Density ($kg\,m^{-3}$)	2100	500	2000	1.2
Specific heat capacity ($J\,kg^{-1}\,K^{-1}$)	900	840	840	1000

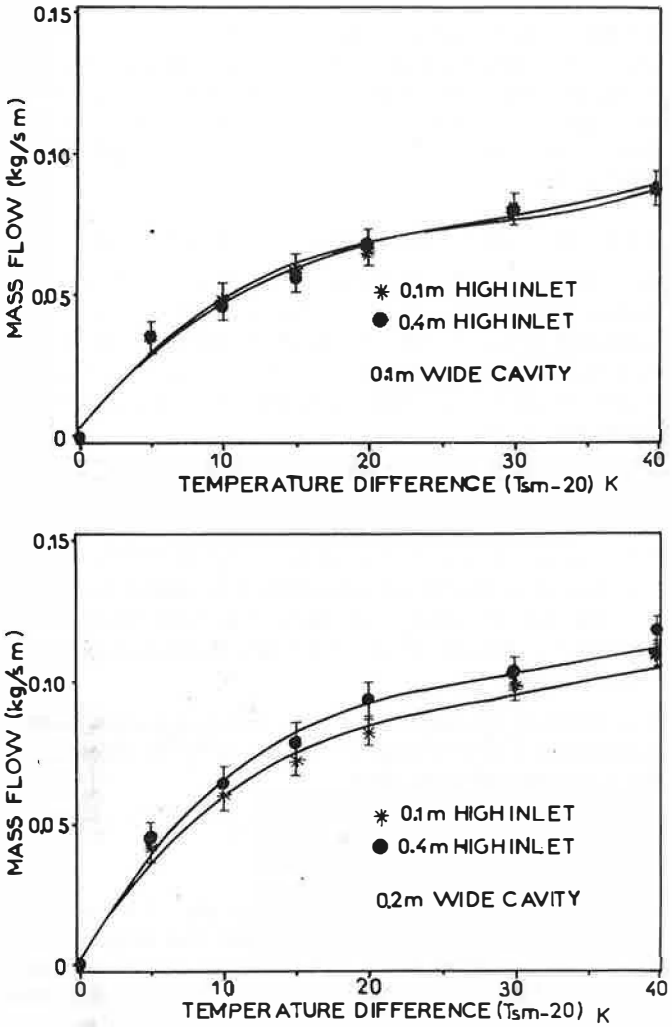

Figure 12 Effect of inlet height on air flow rate for 0.1 m and 0.2 m wide cavities

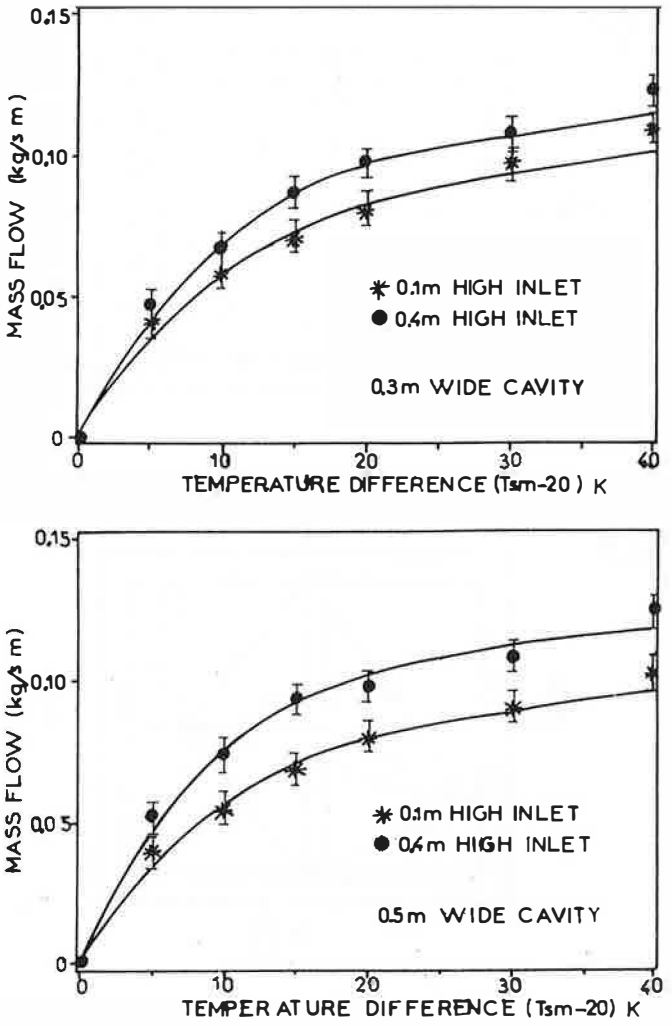

Figure 13 Effect of inlet height on air flow rate for 0.3 m and 0.5 m wide cavities

cavity through the top to the environment was considered negligible because the top opening of the cavity is small compared with the size of the boundary walls.

The dynamic model enabled the response of the cavity within a building under climatic changes with variable boundary conditions to be studied. It was simplified to one-dimensional heat flow equations with a single node for each surface, for the room and the cavity air. It would probably have been more accurate if two-dimensional heat transfer had been used with more nodes throughout the cavity. This would have been more complicated and would have required greater computer storage and running time. The model was simplified further by not considering the effect of intermittent heat inputs from lighting and occupants.

3.3 Finite-difference technique

In order to determine the thermal response of the model, one-dimensional heat flow is assumed and Fourier's differential equation is used. The analytical solution of the Fourier equation is complicated, so a numerical method was used, replacing the differential equation by an equivalent implicit finite-difference one. The implicit method has the advantage that any time increment can be used. In fact, the time increment can be varied during the calculation. It is used in practice when boundary conditions impose small time increments for the stability of the solution. The implicit method has the disadvantage of requiring a complete set of calculations by iteration, Gauss elimination or matrix inversion at each time increment, which may require much computer storage, especially when the number of nodes becomes large. When the boundary conditions involve heat transfer by convection, or by radiation between the surface of the building and its surroundings, the finite-difference equation for nodes at the surface can be obtained by energy balance. In a one-dimensional system, the surface nodes are generally associated with some fraction of mass or capacity from the neighbouring node[10]. Kreith[11] suggested that the volume associated with any surface node is usually taken as half the volume of the next node which is $A\Delta X/2$, where ΔX is the thickness of a slice of the wall. The final result of an implicit method is a set of equations for the future temperature of each node in terms of the present temperature of that node and the future temperatures at neighbouring nodes. There will be as many equations as there are unknown future temperatures. Once this set of equations is solved the resulting future temperature becomes the initial temperature for the next time increment. The implicit method will be stable with any time increment. Its accuracy depends on using the right step and right space increments. The greater the number of nodes and the smaller the time step, the more computer time is used. Nevertheless, Clarke suggested[10] that in building appli-

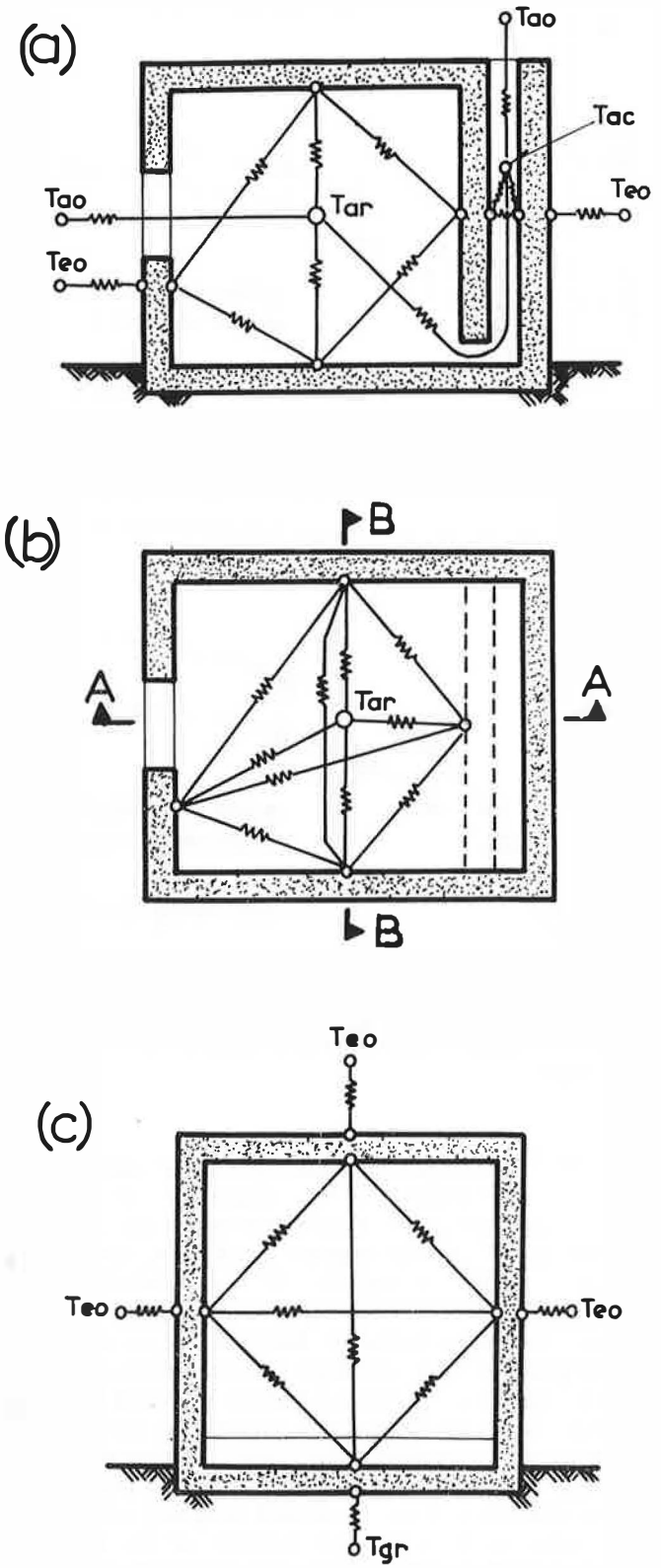

Figure 14 Nodal network for the dynamic model: (a) Section A–A; (b) Plan; (c) Section B–B

cations three nodes per homogeneous element and a time step of an hour are consistent with acceptable accuracy. In the present model, three nodes are used for each slab such as walls, roof and floor. The temperature variation for each single node is evaluated by energy balance. The basis of the heat balance equations is that the algebraic sum of the rate of heat transfer to a node by convection. conduction and radiation must equal the rate of increase of heat content of that node for a given time.

The conditions under which the model was run to give realistic answers were constrained by the climatic conditions of a hot climate. These were; outside air temperature ranging from 15°C to 45°C and surface temperatures varying between 5°C and 75°C. There are four boundary conditions for each case in the present model which are discussed below.

3.4 Heat balance at nodes inside solid building elements

The first boundary condition is obtained from a heat balance within the walls and the bounding surfaces. It is modelled using Fourier's one-dimensional heat conduction equation, where the rate of temperature increase is proportional to the rate of change of temperature gradient, given by:

$$\frac{\partial T}{\partial t} = \frac{\lambda}{\rho c}\frac{\partial^2 T}{\partial x^2} \tag{5}$$

This equation can be solved numerically[11] by dividing the wall into layers of thickness ΔX called nodes, and making a heat balance for each. The heat balance for a node in the middle of the wall is given in the Appendix at equation A1.

The thermal resistance of a slab of homogeneous material is calculated by dividing its thickness by its thermal conductivity and its area, thus:

$$R = \frac{\mathrm{d}x}{A\lambda} \tag{6}$$

where dx is the thickness of the layer and A is one area of the layer (m^2). $R_{so,\,wm}$ is the thermal resistance between the outside surface node and the node in the middle of the wall (m^2KW^{-1}), $R_{si,\,wm}$ is the thermal resistance between the inside surface node and the node in the middle of the wall ($m^2\,KW^{-1}$).

3.5 Heat balance at the external surface nodes

The second boundary condition is obtained from the heat balance equation for the outside surfaces of the model. The external wall exchanges heat with the surrounding surfaces by radiation, with the outside air by convection, and into the wall by conduction. The heat balance for a node exposed to the outside environment according to Kreith[11] is given in Appendix at equation A2.

It is common practice in building energy simulation to represent the external environmental thermal conditions by a single temperature known as the 'sol–air temperature' as defined in the *CIBSE Guide*[2]. The surrounding surfaces are then assumed to be at the outside air temperature. The sol-air temperature is given in the Appendix at equation A3.

3.6 Heat balance at the internal surface nodes

The third boundary condition is obtained from heat balance at any of the inside surfaces of the room and the cavity, where the heat is exchanged by convection with the inside air, by radiation with other surrounding surfaces and by conduction with the walls. The convection heat transfer coefficient used in the room was the one suggested by Alamdari and Hammond[12]. The radiation heat transfer coefficient between the surfaces described in Reference 13 was used. In the cavity, various convection coefficients were used including the one suggested in

the *IHVE Guide*[14], but using the model there was no significant difference in the resulting temperatures. For the radiation heat exchanges in a room or cavity, the room and the cavity are divided into p surfaces. The heat balance at each of the bounding surfaces is given by equation A4 in the Appendix.

3.7 Heat balance for room air and cavity air

The fourth boundary condition is obtained from a heat balance on the room air and the cavity air, where the heat exchange with the air nodes, in the room and in the cavity, takes place by convection with the surrounding surfaces and by ventilation conductance with the outside air.

The heat balance equation for the room air based on Kreith's[11] principle is given as equation A5 in the Appendix. The volume flow rate is equal to the mass flow rate M divided by the air density ρ. The mass flow rate M produced by the temperature difference is determined from the steady-state analysis as given in Reference 8:

$$M = \left(\frac{P_a \rho g Z (T_{ac} - T_{ao})}{287\, C_t (273 + T_{ao})(273 + T_{ac})} \right)^{0.5} \qquad (7)$$

where P_a is the atmospheric pressure (pascal), C_t is a total loss coefficient which can be determined experimentally by dividing the experimentally derived total pressure loss values, for each temperature difference, by the corresponding measured mass flow rates. Tables 2 and 3 show experimental values of C_t under different conditions, when the inlet is 0.1 m and 0.4 m high.

The heat balance for the air node inside the cavity is given by equation A6 in the Appendix.

3.8 Magnitude of mass flow rate

The aim of the sun-warmed cavity is to move as much air as possible. Rates of mass flow were calculated by the above model. The results are plotted in Figure 15 and given in Tables 4, 5 and 6 for a typical cavity (3 m high, 0.20 m wide and 3 m long) with variable external wall thickness facing east, south or west. It is shown that the maximum of rate of ventilation occurs at about 2000 h when the dampers of the cavity are open. Maximum ventilation rates are given in Table 7. This shows that, for a west cavity, as the leaf thickness is increased the mass flow decreases because the thickness of the walls is increased and their mean temperature decreases. The peak ventilation decreases sharply a short time after the opening of the dampers to an average of $0.035\,kg\,s^{-1}\,m^{-1}$. This continues throughout the night until 0800 h when its rate decreases again. At 1000 h the dampers are closed and thus the flow becomes zero.

Table 2 Values of C_t with inlet height 0.1 m

Cavity width (m)	T_{sm} (°C)			
	30	40	50	60
0.1	0.4	0.4	0.4	0.5
0.2	0.6	0.5	0.5	0.5
0.3	0.7	0.6	0.6	0.6

Table 3 Values of C_t with inlet height 0.4 m

Cavity width (m)	T_{sm} (°C)			
	30	40	50	60
0.1	5.0	2.8	1.8	2.2
0.2	5.4	3.4	4.7	4.0
0.3	7.7	5.1	6.7	5.5

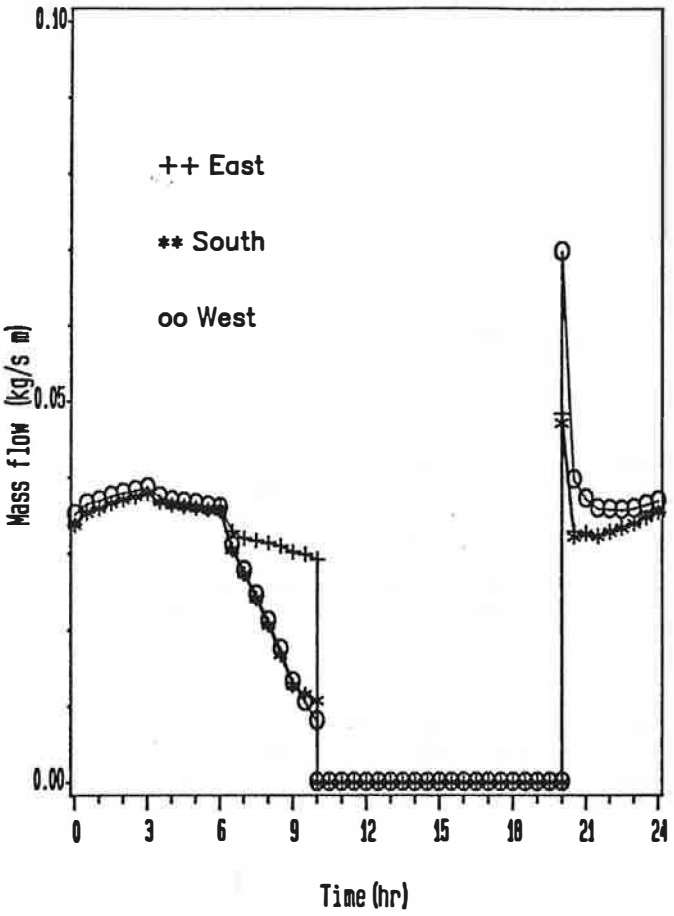

Figure 15 Mass flow per unit length with 0.05 m thick external wall of the cavity

In order to compare the mass flow rates obtained from the dynamic model and experiment, typical values were taken. From the model, considering a time of 2000 h the mean surface temperature of the cavity was 44°C and the outside temperature of the air was 34°C, with a temperature difference of 10 K. This gave a mass flow rate of $0.07\,kg\,m^{-1}\,s^{-1}$. From experimental work, considering similar temperatures, the mass flow was $0.06\,kg\,m^{-1}\,s^{-1}$. The two values can be seen to agree closely.

Consider a second example. From the dynamic model at 0650 h, a temperature difference of 5 K was predicted between the surfaces of the cavity and the outside air. This gave a mass flow of $0.032\,kg\,m^{-1}\,s^{-1}$. From measured data at the same temperature difference a mass flow of $0.043\,kg\,m^{-1}\,s^{-1}$ was obtained.

3.9 Optimum azimuth

The azimuth at which a sun-warmed cavity would give the best performance must be known. The south might be thought 'the best azimuth' for a sun-warmed cavity or solar chimney, but this is not so in low latitudes. Results plotted in Figure 15 and given in Tables 4, 5 and 6 show the comparison of the rates of mass flows in cavities with azimuths East, South and West for a latitude 33°N.

Table 4 Mass flow per unit length ($kg\,s^{-1}\,m^{-1}$) with external wall of cavity 0.1 m thick

Direction	Time (h)											
	0	2	4	6	8	10	12	14	16	18	20	22
East	0.035	0.038	0.038	0.036	0.026	0.021	0.000	0.000	0.000	0.000	0.052	0.035
South	0.035	0.038	0.038	0.036	0.021	0.000	0.000	0.000	0.000	0.000	0.050	0.035
West	0.037	0.040	0.039	0.037	0.022	0.000	0.000	0.000	0.000	0.000	0.071	0.038

Table 5 Mass flow per unit length with external wall of cavity 0.15 m thick

Direction	Time (h)											
	0	2	4	6	8	10	12	14	16	18	20	22
East	0.036	0.040	0.039	0.037	0.024	0.013	0.000	0.000	0.000	0.000	0.051	0.035
South	0.036	0.040	0.039	0.037	0.022	0.000	0.000	0.000	0.000	0.000	0.047	0.033
West	0.0387	0.041	0.040	0.039	0.023	0.000	0.000	0.000	0.000	0.000	0.063	0.038

Table 6 Mass flow per unit length with external wall of cavity 0.20 m thick

Direction	Time (h)											
	0	2	4	6	8	10	12	14	16	18	20	22
East	0.036	0.040	0.040	0.039	0.024	0.006	0.000	0.000	0.000	0.000	0.047	0.035
South	0.036	0.040	0.040	0.039	0.023	0.000	0.000	0.000	0.000	0.000	0.041	0.034
West	0.038	0.041	0.041	0.040	0.024	0.000	0.000	0.000	0.000	0.000	0.053	0.037

Table 7 Maximum mass flow rates ($kg\,s^{-1}\,m^{-1}$) for a typical cavity

Cavity orientation	External wall thickness (m)			
	0.05	0.10	0.15	0.20
East	0.048	0.052	0.051	0.047
South	0.047	0.050	0.047	0.041
West	0.069	0.071	0.063	0.053

From these results it is clear that a cavity facing west produces higher mass flow in the evening (from 2000 h to 2400 h). The fact that the west azimuth is preferred results from the fact that at low latitudes such as 33.3°N, the total solar radiation received on a west wall is much more than the other azimuths[13].

3.10 Optimum leaf thicknesses

In hot climates buildings usually have walls from 0.3 m to 0.5 m thick. In the application of a sun-warmed cavity, the internal leaf generally has a fixed thickness between 0.2 m and 0.3 m. In this study the outer leaf is made variable. If the outer leaf is thicker, more heat can be stored, but this would result in the decline of the cavity mean air temperature. If the leaf is made thinner, less heat can be stored and the cavity life would be shorter. Consequently there must be an optimum performance thickness. Tables 8, 9 and 10 compare mass flow rates of air produced by a cavity of various external leaf thicknesses with different azimuths. Although the differences between the results are not significant, there is an indication that the thicker the external leaf of the cavity, the

Table 8 Mass flow per unit length ($kg\,s^{-1}\,m^{-1}$) produced by an East-facing cavity

External wall thickness (m)	Time (h)											
	0	2	4	6	8	10	12	14	16	18	20	22
0.05	0.033	0.037	0.037	0.036	0.031	0.030	0.000	0.000	0.000	0.000	0.048	0.034
0.10	0.035	0.038	0.038	0.036	0.026	0.021	0.000	0.000	0.000	0.000	0.052	0.035
0.15	0.036	0.040	0.039	0.037	0.024	0.013	0.000	0.000	0.000	0.000	0.051	0.035
0.20	0.036	0.040	0.040	0.039	0.025	0.006	0.000	0.000	0.000	0.000	0.053	0.037

Table 9 Mass flow per unit length ($kg\,s^{-1}\,m^{-1}$) produced by a South-facing cavity

External wall thickness (m)	Time (h)											
	0	2	4	6	8	10	12	14	16	18	20	22
0.05	0.033	0.037	0.037	0.036	0.021	0.011	0.000	0.000	0.000	0.000	0.047	0.034
0.10	0.035	0.038	0.038	0.036	0.021	0.000	0.000	0.000	0.000	0.000	0.050	0.035
0.15	0.036	0.040	0.039	0.037	0.022	0.000	0.000	0.000	0.000	0.000	0.047	0.033
0.20	0.036	0.040	0.040	0.039	0.023	0.000	0.000	0.000	0.000	0.000	0.041	0.034

Table 10 Mass flow per unit length ($kg\,s^{-1}\,m^{-1}$) produced by a West facing cavity

External wall thickness (m)	Time (h)											
	0	2	4	6	8	10	12	14	16	18	20	22
0.05	0.035	0.038	0.037	0.036	0.021	0.008	0.000	0.000	0.000	0.000	0.069	0.036
0.10	0.037	0.040	0.039	0.037	0.022	0.000	0.000	0.000	0.000	0.000	0.071	0.038
0.15	0.038	0.041	0.040	0.039	0.023	0.000	0.000	0.000	0.000	0.000	0.063	0.038
0.20	0.038	0.041	0.041	0.040	0.024	0.000	0.000	0.000	0.000	0.000	0.053	0.037

higher the rate of mass flow from 2400 h until 0900 h will be. In the evening up to 2400 h, when the damper is open, the trend of the results is different. A 0.20 m thick leaf gives low ventilation whereas a 0.10 m thick cavity leaf gives a slightly better value. This indicates that the optimum thickness of the outer leaf of a cavity lies between 0.10 m and 0.15 m. Economically, reducing the amount of material used is desirable, consequently a 0.10 m leaf on the outside of the cavity may be the best.

3.11 Cooling effect

In order to assess the cooling in a typical room with a typical cavity, room air temperatures were calculated when the dampers are closed all day with low ventilation and when air flow in the cavity is permitted in the evening, because the dampers are open.

Figure 16 shows the room air temperatures for the two cases. The corresponding sol–air and outside air temperatures are also shown. It can be seen that the room air temperature was reduced by about 5 K in the latter circumstance.

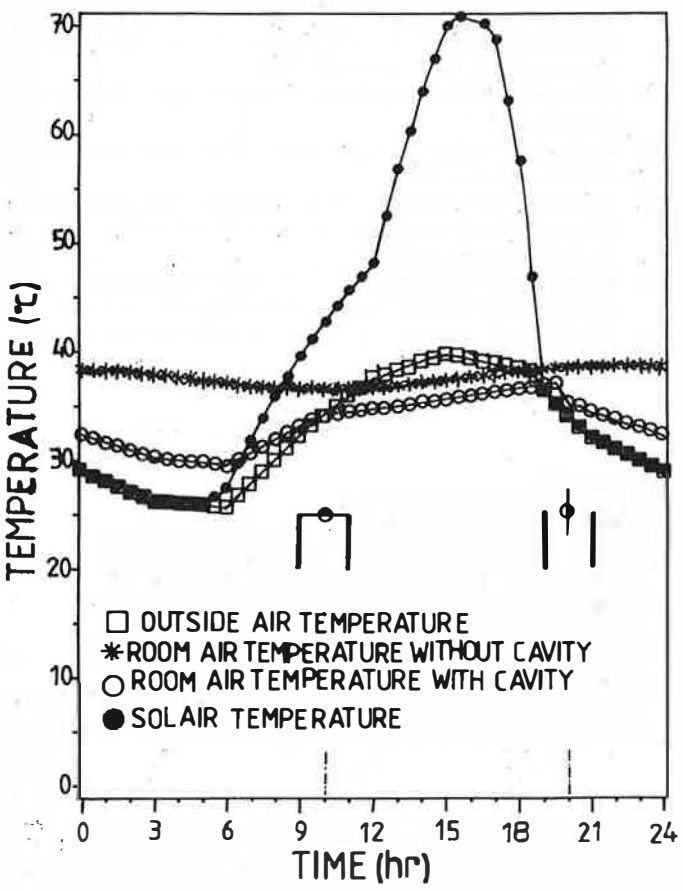

Figure 16 Room air temperature with west facing cavity

Comparison with other models is very limited because of lack of data in the literature for similar cases. However, Yagoubi and Golneshan[1] studied the effect of cross ventilation at night on room air temperature using a wind tower in a hot climate. Ventilation was allowed from 2300 h to 0600 h. They showed that with a rate of 12 air changes per hour, the room temperature is reduced by an average of 2 K during the day, with a maximum reduction of about 4 K. This is not far from our values.

The dynamic model showed that an average mass flow rate of $0.035\,kg\,s^{-1}$ is achieved for a 1 m long heated cavity, 0.2 m wide. For a 3 m long cavity, this would be three times greater, about $0.1\,kg\,s^{-1}$ if we assume that the air travels mainly in stream lines through the room into the cavity, as shown experimentally. This would result in an air speed of $0.15\,m\,s^{-1}$. When the cavity is open, the mass flow is at its highest value of $0.071 \times 3\,kg\,s^{-1}$ giving an air velocity of $0.3\,m\,s^{-1}$. Without the cavity, the dynamic model showed a high resultant temperature between 36 and 39°C. With the cavity the resultant temperature decreased to the range of 32 to 36°C, an improvement of 3 to 4 K.

3.12 Best time to open dampers

In order to know the best time for opening the dampers of a sun-warmed cavity for ventilation, a range of times were selected. Figure 17 shows how the room air temperature changes when the damper is opened at different times. Ventilation from 2000 h to 1000 h gives a lower room air temperature than ventilation from 2200 h to 1000 h or from 2400 h to 1000 h. There is no difference between the results when ventilation is allowed from 2000 h to 0800 h. This suggests that for improving cooling, ventilation at night should be prolonged for as long as the outside temperature is comfortable.

The results presented here are based on climatic data for El-Oued where the outside air temperature at night is high. In most hot climates, where the outside air temperature at night is lower, cooling with ventilation will be more effective.

4 Conclusions

This study suggests that thermal comfort can be improved by using a sun-warmed cavity to promote ventilation during the night. It was shown that a warm layer developed over each heated surface and when these layers interacted the air flow was almost entirely upwards through the cavity which was desirable. When the layers were discrete with no overlapping, there was down flow in the central section which decreased the rate of air flow through the room. For a 2 m high cavity and an inlet height of 0.1 m, the optimum cavity width was about 0.2 m. With higher cavities the optimum width would be wider.

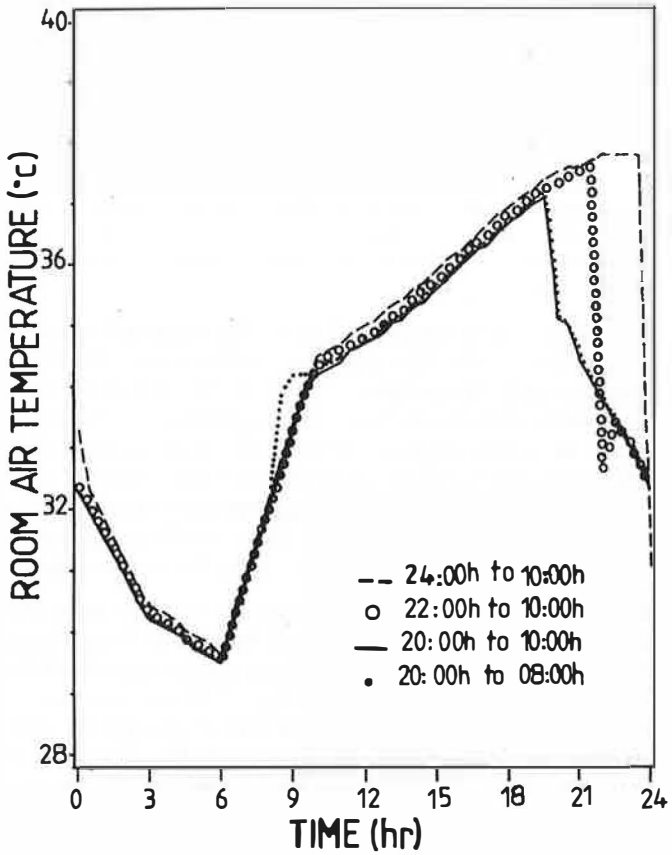

Figure 17 Effect of opening times of damper on room air temperature

The experimental results also showed that for a temperature difference of 5 K between the cavity surface and incoming air, a mass flow rate of about $0.043\,kg\,m^{-1}\,s^{-1}$ could be achieved. This value would be three times greater if the cavity were 3 m long. The air velocity achieved by this mass flow rate is in the order of $0.36\,m\,s^{-1}$ through the room. Such a velocity would reduce the resultant temperature to a comfortable region.

Data from a computer model indicated that if a sun-warmed cavity or 'solar chimney' is to be used to induce evening ventilation in buildings in low latitudes, its best location is on a west wall. Such positioning also reduces heat storage time required before the cavity is opened.

Results from the dynamic model showed that the optimum thickness of the outer leaf is between 0.1 m and 0.15 m.

The model predicted that for a typical room in a hot climate, with a cavity facing west, a maximum ventilation rate of $0.07\,kg\,s^{-1}$ could be obtained with a cavity 1 m long and 3 m high. An average value would be $0.035\,kg\,s^{-1}$ over the time the cavity was opened. If the cavity were extended the full length of a wall while operational, the flow rate would be three times greater. This would induce air speed across the room of about $0.29\,m\,s^{-1}$. Without the sun-warmed cavity, the resultant temperature in the room would be in the range of 36–38°C. With the cavity increasing the air speed across the room the resultant temperature would be reduced to between 32 and 36°C which is comfortable.

When building a sun-warmed cavity on a dwelling in a hot climate, maximum ventilation will be achieved by following appropriate guidelines as follows:

(*a*) orienting the cavity westward at low latitudes near the equator.

(*b*) constructing long cavities so that more heat is stored. However, this may occasionally be an uneconomic use of materials and be impracticable.

(*c*) optimising the width of the cavity in relation to its height using the relationship $W_{optimum} = Z/10$.

(*d*) extending the inlet along the length of the cavity to maximise air entry.

(*e*) constructing the outer (wall) 0.1 m to 0.15 m thick.

References

1 Yagoubi M A and Golneshan A A Passive cooling of an underground room (Sardab) *Iranian J. Sci. Technol.* **10**(1&2) 89–98 (1986)

2 *CIBSE Guide* Volume A (London: Chartered Institution of Building Services Engineers) (1986)

3 Nicol J F *An analysis of some observations of thermal comfort in Roorkee, India and Baghdad, Iraq* (Garston: Building Research Establishment) (1975)

4 Koenigsberger O H, Ingersoll T G, Mayhew A and Szokolay S V *Manual of tropical housing and building: Climatic design* (London: Longman) (1974)

5 Evans M *Housing climate and comfort* (London: Architectural Press) (1980)

6 Olgyay V *Design with climate—Bioclimatic approach to architectural regionalism* (Princeton: Princeton University Press) (1963)

7 Bouchair A *Solar induced ventilation in the Algerian and similar climates* PhD thesis, University of Leeds (1989)

8 Bouchair A, Fitzgerald D and Tinker J A Passive solar induced ventilation *Proc. Miami international Conference on Alternative Energy Sources* (8th 1987: Palm Beach, Florida) *Alternative energy sources VIII* ed. T Nejat Viziroglu (New York: Hemisphere) (1989)

9 Bouchair A, Fitzgerald D and Tinker J A Moving air using stored solar energy *Proc. 13th National Passive Solar Conference, Cambridge, MA* ASES pp 33–38 (1988)

10 Clarke A I *Energy simulation in building design* (Bristol: Adam Hilger) (1985)

11 Kreith F *Principles of heat transfer* (New York: Intext Educational Publishers) (1973)

12 Alamdari F and Hammond G P Improved data correlations for buoyancy-driven convection in rooms *Building Serv. Eng. Res. Technol.* **4** (3) 106–12 (1983)

13 Bouchair A and Fitzgerald D The optimum azimuth for a solar chimney in hot climates *Energy and Buildings* **12**(2) 135–140 (1988)

14 *IHVE Guide* (London: Institute of Heating and Ventilating Engineers) (1970)

Appendix

$$\frac{T_{so}^{t+1} - T_{wm}^{t+1}}{R_{so,,\,wm}} + \frac{T_{si}^{t+1} - T_{wm}^{t+1}}{R_{si,\,wm}} = \frac{(\rho c V)_{wm}}{\Delta T}(T_{wm}^{t+1} - T_{wm}^{t}) \qquad \text{(A1)}$$

$$\frac{T_{eo}^{t+1} - T_{so}^{t+1}}{R_{eo,\,so}} + \frac{T_{wm}^{t+1} - T_{so}^{t+1}}{R_{wm,\,so}} = \frac{(\rho c V)_{so}}{\Delta T}(T_{so}^{t+1} - T_{so}^{t}) \qquad \text{(A2)}$$

$$T_{eo} = T_{ao} + R_{eo,\,so}(\alpha I_{tvd} - EI_{l}) \qquad \text{(A3)}$$

where

$$R_{\mathrm{eo,\,so}} = \frac{1}{(Eh_{\mathrm{r}} + h_{\mathrm{c}})}$$

and $R_{\mathrm{eo,\,so}}$ is the combined outside surface resistance ($\mathrm{m^2\,K\,W^{-1}}$), E is the surface emissivity, α is the surface absorptivity, I_{l} is the long-wave radiation loss ($\mathrm{W\,m^{-2}}$), I_{tvd} is the total solar radiation ($\mathrm{W\,m^{-2}}$), V_{so} is the volume of a layer ($\mathrm{m^3}$).

$$\frac{T_{\mathrm{wm}}^{t+1} - T_{\mathrm{si}}^{t+1}}{R_{\mathrm{wm,\,si}}} + \frac{T_{\mathrm{ar}}^{t+1} - T_{\mathrm{si}}^{t+1}}{R_{\mathrm{ar,\,si}}} + \sum_{p=1}^{p=n} \frac{T_p^{t+1} - T_{\mathrm{si}}^{t+1}}{R_{p,\,\mathrm{si}}} = \frac{(\rho cV)_{\mathrm{si}}}{\Delta T}(T_{\mathrm{si}}^{t+1} - T_{\mathrm{si}}^{t}) \qquad \text{(A4)}$$

where $\sum_{p=1}^{p=n}$ is for the radiation part between the surfaces, $R_{\mathrm{ar,\,si}}$ is the convective thermal resistance between the air node and inside the surface node ($\mathrm{m^2\,K\,W^{-1}}$), $R_{p,\,\mathrm{si}}$ is the radiation thermal resistance between inside surface nodes ($\mathrm{m^2\,K\,W^{-1}}$).

$$\sum_{m=1}^{m=n} \frac{T_m^{t+1} - T_{\mathrm{ar}}^{t+1}}{R_{\mathrm{m,\,ar}}} + [(T_{\mathrm{ao}}^{t+1} - T_{\mathrm{ar}}^{t+1}) + (T_{\mathrm{ac}}^{t+1} - T_{\mathrm{ar}}^{t+1})]C_{\mathrm{v}} = \frac{(\rho cV)_{\mathrm{ar}}}{\Delta T}(T_{\mathrm{ar}}^{t+1} - T_{\mathrm{ar}}^{t}) \qquad \text{(A5)}$$

where $R_{\mathrm{m,\,ar}}$ is the thermal resistance by convection between the inside surface nodes of the room and the air in the room ($\mathrm{m^2K\,W^{-1}}$), C_{v} is the ventilation conductance (the reciprocal of the ventilation resistance) given by:

$$C_{\mathrm{v}} = \rho cV_{\mathrm{f}}$$

and V_{f} is the volume flow rate ($\mathrm{m^3\,s^{-1}}$)

$$\sum_{p=1}^{p=n} \frac{T_p^{t+1} - T_{\mathrm{ac}}^{t+1}}{R_{p,\,\mathrm{ac}}} + [(T_{\mathrm{ao}}^{t+1} - T_{\mathrm{ac}}^{t+1}) + (T_{\mathrm{ar}}^{t+1} - T_{\mathrm{ac}}^{t+1})]C_{\mathrm{v}} = \frac{(\rho cV)_{\mathrm{ac}}}{\Delta T}(T_{\mathrm{ac}}^{t+1} - T_{\mathrm{ac}}^{t}) \qquad \text{(A6)}$$

length of the cavity width. Mass flow rates were determined by multiplying the following parameters measured at the air inlet: average air velocity $\bar{v}(\mathrm{m\,s^{-1}})$, air density $\rho(\mathrm{kg\,m^{-3}})$ and area of inlet $A(\mathrm{m^2})$. To determine the mass flow rate per unit length, the value obtained was simply divided by the length of the cavity. For each surface temperature, cavity width and inlet height a mass flow rate per unit length was calculated. The results are plotted in Figure 2. It has been observed that the mass flow rate maximises when the cavity width is between 0.2 and 0.3 m. Increasing the cavity width (for the 0.1 m and 0.4 m high inlets) from 0.3 to 1.0 m shows a decline in the mass flow rates which suggests that increasing the cavity width above 0.3 m may not be beneficial.

The graphs also show that increasing the surface temperature increases the mass flow rate. This can be explained by the fact that with high surface temperatures, the air within the cavity gets hotter, thereby reducing its density and increasing the buoyancy pressure.

The above observations were based on measurements taken at the air inlet to the cavity. For continuity through the whole system, the mass flow rate of air must be constant. Mass balances were carried out at the window, the inlet and the outlet to the cavity for each cavity width and surface temperature value. To do this the cavity width was varied as 0.1 m, 0.2 m, 0.3 m, 0.5 m and surface temperatures increased by 5 K to 40 K above the ambient air temperature at each width. The ambient air temperature was kept constant at 20°C. The inlet height was initially 0.1 m, and was then increased to 0.4 m. The results are plotted in Figures 3 to 6.

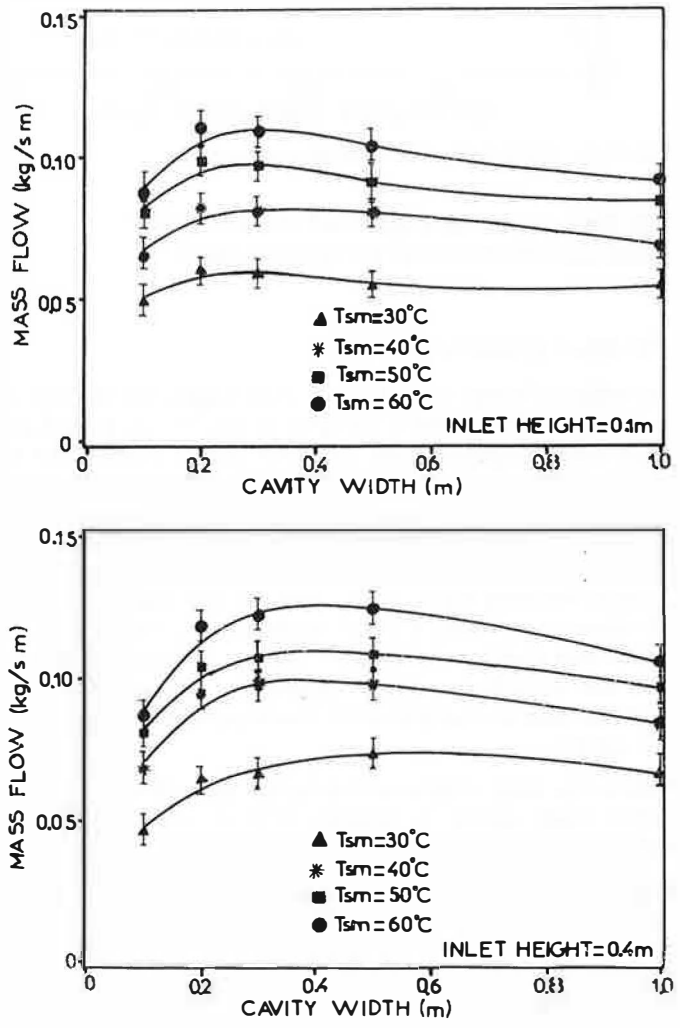

Figure 2 Effect of cavity width on air flow rate

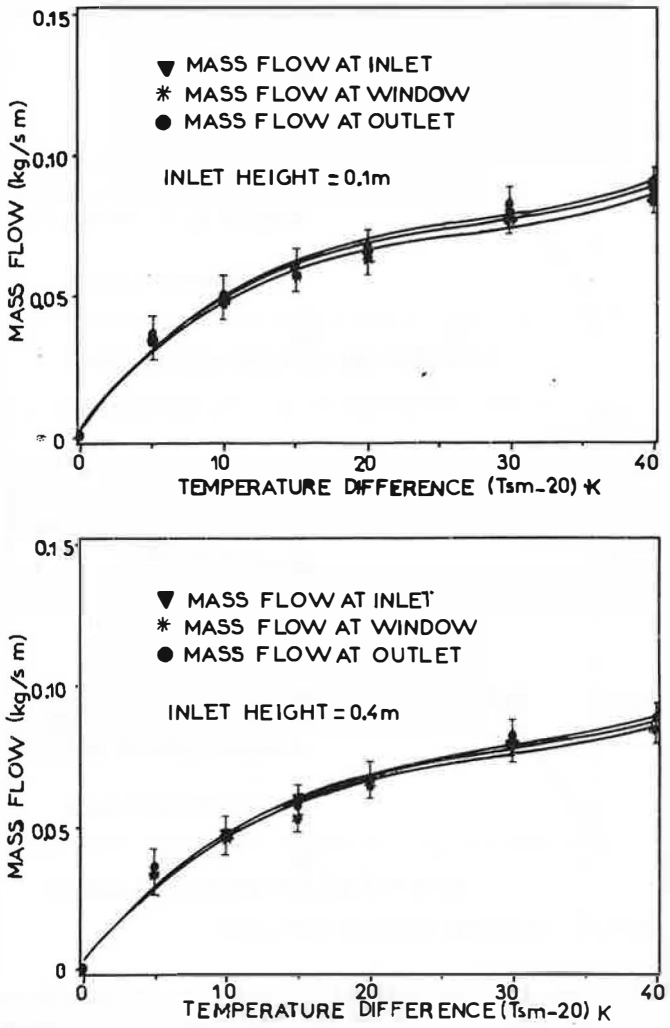

Figure 3 Mass balance for 0.1 m wide cavity

Statistical analysis of the data shows that the regression lines plotted in Figure 3 are quite close to one another. The error bars of the data overlap to such an extent that the curves could be assumed to be the same. This closeness of fit suggests that the mass flow rates of the air at the inlet, window and outlet are the same. The same explanation could be given for the data of Figures 4 and 5. For a cavity of width 0.5 m, the statistics show that the mass flow rate at the outlet was higher than at the inlet and window (Figure 6). The mass flow at the inlet and the window are similar. The reason why the mass flow rates are higher at the outlet than at the inlet and window is additional air entering the system. Knowing that the thermistor anemometer used in these measurements indicates the speed of air but not its direction, it was necessary to use smoke to identify the flow patterns and to see where the additional air came from.

2.2 Air flow patterns

The use of smoke enabled the air flow patterns in the cavity and in the room to be traced at various places.

Within the cavity, smoke was injected horizontally in various places at the top. If there is no up or down flow,

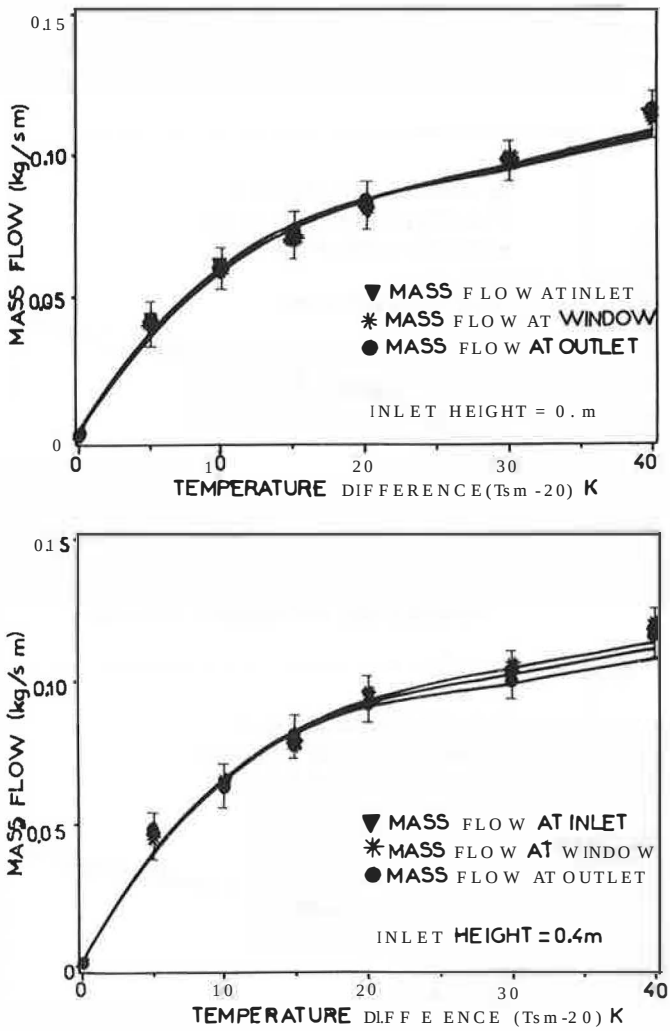

Figure 4 Mass balance for 0.2 m wide cavity

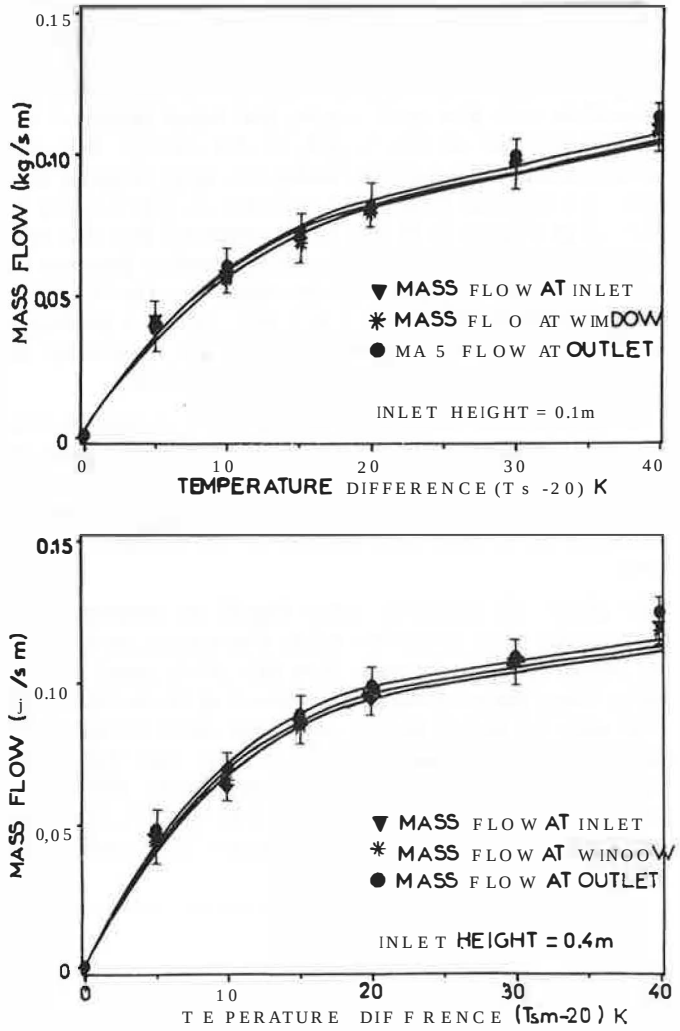

Figure 5 Mass balance for 0.3 m wide cavity

the smoke will move slowly, horizontally. If there is up or down flow then the smoke will migrate accordingly. The cavity was varied in width as 0.1 m, 0.2 m, 0.3 m, 0.5 m. For 0.1 m, 0.2 m and 0.3 m wide cavities the smoke trace was observed to be entirely upwards (Figure 7). This confirms the mass flow results reported previously.

With a 0.5 m wide cavity, the smoke moved downwards in the central section of the cavity, whereas it was upwards within a section about 125 mm thick from each side of the cavity (Figures 8 and 9). The upward air flow on either side was supplied from the room through the inlet, and partly from down flow in the centre of the cavity. Figure 10 is a schematic diagram of the possible flow patterns in a 0.5 m wide cavity.

In the room, similar observations were made to check the direction of through-flow of air to see whether there was any reverse flow from the room to the outside via the window, and also to see how the air passed through the room into the cavity. Observations also made it possible to see whether the air filled the whole room before it migrated into the cavity or whether it passes in a stream line directly to the inlet. Smoke was injected initially through the window and then through the inlet (Figure 11). It was observed that air travelled through the room in a stream line from the window towards the inlet and then to the heated cavity. There was no reverse flow. Smoke traces below and above the window were almost stagnant, indicating that the flow does not affect the whole of the air in the room. This indicates that the windows should be positioned in such a way that ventilation can affect most of the internal space.

2.3 *Effect of inlet height*

In order to know the effect of inlet height on the rate of mass flow, flows were monitored for 0.1 m and 0.4 m high inlets together with different cavity widths (0.1 m, 0.2 m, 0.3 m and 0.5 m). The surface temperature was increased from 5 K to 40 K above the ambient air temperature. Results are plotted in Figures 12 and 13, which show the mass flow rate as a function of temperature difference between surfaces T_{sm} and the entering air. Figure 12 shows that with a 0.1 m wide cavity, the curves for 0.1 m and 0.4 m inlet heights are very close, suggesting that the inlet has no effect on the rate of mass flow, and that the flow is dominated by frictional losses throughout the cavity.

When the inlet height is 0.4 m, the mass flow rate for a 0.2 m wide cavity is slightly higher, indicating some influence of inlet height on mass flow rate.

Figure 13 shows that as the cavity is increased to 0.3 m and 0.5 m, the inlet height begins to show a more pronounced influence on the mass flow rate. More mass flow is produced with a high inlet. In such cases the frictional losses inside the cavity are negligible and thus the pressure loss at the inlet becomes significant. When the inlet is increased, more mass flow is allowed through the inlet